



HAL
open science

Microplastics in the maximum chlorophyll layer along a north-south transect in the Mediterranean Sea in comparison with zooplankton concentrations

François Carlotti, Olivia G rigny, Dorian Bienvenu, Christophe Ravel, Pamela Fierro-Gonz lez, Lo c Guilloux, Nouha Makhoul, Javier Tes n Onrubia, Marc Pagano

► To cite this version:

Fran ois Carlotti, Olivia G rigny, Dorian Bienvenu, Christophe Ravel, Pamela Fierro-Gonz lez, et al.. Microplastics in the maximum chlorophyll layer along a north-south transect in the Mediterranean Sea in comparison with zooplankton concentrations. *Marine Pollution Bulletin*, 2023, 196, pp.115614. 10.1016/j.marpolbul.2023.115614 . hal-04269744

HAL Id: hal-04269744

<https://hal.science/hal-04269744>

Submitted on 3 Nov 2023

HAL is a multi-disciplinary open access archive for the deposit and dissemination of scientific research documents, whether they are published or not. The documents may come from teaching and research institutions in France or abroad, or from public or private research centers.

L'archive ouverte pluridisciplinaire **HAL**, est destin e au d p t et   la diffusion de documents scientifiques de niveau recherche, publi s ou non,  manant des  tablissements d'enseignement et de recherche fran ais ou  trangers, des laboratoires publics ou priv s.

1
2
3
4
5
6
7 **Microplastics in the maximum chlorophyll layer along a north-south transect in the**
8 **Mediterranean Sea in comparison with zooplankton concentrations**
9

10
11
12
13
14
15
16 **François Carlotti ^{a*}, Olivia G rigny ^b, Dorian Bienvenu ^a, Christophe Ravel ^b,**
17
18 **Pamela Fierro-Gonz lez ^a, Lo c Guilloux ^a, Nouha Makhoulouf ^{a,c}, Javier Tes n Onrubia ^a, Marc**
19
20 **Pagano ^a**
21
22
23
24

25
26 **^a Aix Marseille Univ, Universit  de Toulon, CNRS, IRD, MIO UM 110, 13288, Marseille,**
27 **France**
28

29 **^b Ifremer, ODE/UL/LER-PAC, La Seine-sur-Mer, France**
30

31 **^c Universit  de Carthage Facult  des Sciences de Bizerte, Zarzouna, 7021, Tunisia**
32
33
34
35
36
37
38
39
40
41

42
43 *** Corresponding author:**
44

45 E-mail address: francois.carlotti@mio.osupytheas.fr
46
47
48
49
50
51
52
53
54
55
56
57
58
59
60
61
62
63
64
65

Microplastics in the maximum chlorophyll layer along a north-south transect in the Mediterranean Sea in comparison with zooplankton concentrations

The aim of this study was to characterize and quantify microplastics (MPs) at the chlorophyll maximum layer (CML), around 30 to 60 m depth, during a cruise dedicated to the study of contaminants in plankton, the MERITE-HIPPOCAMPE project, along a north-south transect in the western Mediterranean Sea (Tedetti et al., 2023). Plankton were collected by horizontal net tows in this layer using a multinet Hydrobios Midi equipped with 60 μm mesh-size nets. The collected plankton were fractionated through a sieve column for various later contaminant measurements and for zooplankton analysis (Fierro-González et al., 2023). For all stations, samples were also fully examined for microplastics (MPs) for fractions greater than 300 μm . MPs were found at all stations in the CML layer (mean: 42.9 ± 45.4 MPs m^{-3}), of which $96 \pm 4\%$ were fibers. The ratios of mesozooplankton/MPs and detritus/MPs in this CML were respectively 223 ± 315 and 2544 ± 2268 . These data are analyzed together with MPs concentrations from sea- surface sampled with a 300 μm net-size Manta net at the same stations. Overall, our observations highlight the very high density of fibers at the CML, mainly associated with aggregates, raising the hypothesis of their interactions with marine snow. Therefore, the importance of marine snow and vertical layering will have to be considered in future MP distribution modelling efforts.

Keywords: (maximum 5): Microplastics, Mediterranean Sea, chlorophyll maximum, zooplankton, detritus

Highlights

- High MPs densities observed at the chlorophyll maximum layer in Mediterranean Sea
- Fibers were the dominant MPs at the CML
- Fibers were mostly associated with detritus in aggregates
- At the CML, zooplankton/MPs ratio varied from 5 to 1000

1. Introduction

1
2 MPs in the oceans are assessed as a growing threat to marine food chains (Cole et al., 2011).
3
4 The vast majority of observations of MPs in the ocean environment are made at the surface
5
6 and on the seabed substrate, and much less in the water column (Cincinelli et al., 2019;
7
8 Lefebvre et al., 2019; Chevalier et al., 2023), even though the redistribution of surface MPs
9
10 in the first 10 meters of the water column by mixing due to wind stress has received more
11
12 attention in order to correct assessments of surface MPs concentrations (Kukulka et al.,
13
14 2012; Chevalier et al. 2023 and quoted references therein). Numerous studies have been
15
16 carried out on the sedimentation of surface MPs, mostly using modelling or experimental
17
18 approaches, even including the impact of potential degradation and biofouling processes
19
20 (e.g., Mendrik et al., 2023). To date, very few studies have attempted to quantify variations
21
22 in the distribution of MPs in the water column (Choy et al., 2019, in offshore areas; Chevalier
23
24 et al., 2023 in inshore areas), and they have highlighted accumulation layers. The fate of MPs
25
26 in the pelagic food chain is also of great interest, as the size spectrum of MPs ranges from
27
28 hundreds of μm to a few mm, and shows a strong overlap with the size spectrum of
29
30 planktivorous fish prey (Chen et al., 2022). However, potential risks for planktivorous fishes
31
32 ingesting MPs are inferred from potential predation at the surface (e.g., Fabri-Ruiz et al.,
33
34 2023), while major trophic interactions occur on zooplankton patches within the water
35
36 column (Benoit-Bird, 2009; Möller et al., 2012). Studies combining MPs sampling within
37
38 layers of the water column and observation in planktivorous fish guts are still very rare
39
40 (Lefebvre et al., 2019). In the marine environment, the water column is also the site of an
41
42 abundant load of particles, called 'marine snow', composed of aggregates of organic and
43
44 inorganic matter, whose size spectrum ranges from 0.5 mm to tens of cm (Alldredge and
45
46 Silver, 1988), strongly overlapping with the MPs size spectrum. This marine snow is also
47
48
49
50
51
52
53
54
55
56
57
58
59
60
61
62
63
64
65

1 characterized by layers of higher density within the water column (Möller et al., 2012). How
2 marine snow interacts with MPs is unknown. Therefore, it is essential to know and quantify
3 the MPs that can be found in key layers of the water column, together with the associated
4 concentrations of zooplankton and detritus.
5
6
7
8
9

10 In order to better understand the role of plankton as a pump of contaminants, the MERITE-
11 HIPPOCAMPE project (Tedetti et al., 2023) has developed a massive sampling protocol at the
12 chlorophyll maximum layer (CML). Zooplankton sampling was carried out by horizontal tows
13 of nets through filtration of large volumes. This approach provided a unique opportunity to
14 examine the MPs content in samples intended for counting and characterizing the collected
15 zooplankton (Fierro-González et al., 2023). The **aims of this study** were (1) to count, classify
16 and measure MPs collected at the CML during the MERITE-HIPPOCAMPE cruise, (2) to
17 identify differences in concentrations and size structures between the MPs collected at the
18 CML and those collected at the sea surface, (3) to compare the concentrations of MPs to
19 zooplankton and detritus densities in the same samples, (4) to identify potential differences
20 between the coastal and offshore stations.
21
22
23
24
25
26
27
28
29
30
31
32
33
34
35
36
37
38
39
40

41 **2. Material and methods**

42
43
44 **Study area and environmental data.** The MERITE-HIPPOCAMPE cruise was carried out
45 between 13 April and 14 May 2019, along a north-south transect in the western
46 Mediterranean Sea, from the French coast (Toulon, Marseille) to the Tunisian coast (Gulf of
47 Gabès) aboard the French Research Vessel *Antea* (see **Fig. 2** in Tedetti et al., 2023). Ten
48 stations were sampled from the bays of Toulon and Marseille in the north (4 north coast
49 stations: St 01: coastal station in the inner bay of Toulon; St 02: station offshore of the bay of
50 Toulon; St 03: offshore of the bay of Marseille, above the head of the Planier Canyon on the
51
52
53
54
55
56
57
58
59
60
61
62
63
64
65

1 shelf break; and St 04 within the bay of Marseille) to the south of the Tunisian continental
2 shelf (3 south coast stations: St15 in the Gulf of Hammamet, St17 and St19 in the Gulf of
3 Gabes), with three deep oceanic stations along the transect, one in the Ligurian Sea (St09
4 offshore station to the north of the Balearic Thermal Front) and two stations west of the
5 Sardinian coasts (St10 is situated southwards of the Balearic Front and north of Sardinia, and
6 St11 southwest of Sardinia). For each station, the date of sampling, the geographical position,
7 the station depth, and the depth of the different samples (CTD and net tows explained below)
8 are presented in **Table 1** in Tedetti et al. (2023). At each station, an oceanographic carousel
9 equipped with a CTD Seabird SBE 911+ to measure the hydrological variables (temperature,
10 density and salinity) was deployed down to 250 m for open-sea stations or near the bottom
11 for shallower stations. In addition, the CTD was coupled with several sensors including
12 chlorophyll-a fluorescence (Chla; Aqua Tracka, Chelsea ctg), LISST and LOPC optical sensors.
13
14
15
16
17
18
19
20
21
22
23
24
25
26
27
28
29
30

31 ***Zooplankton and MPs sampling and observations.*** Micro- and mesoplankton were sampled
32 with a Multiple Plankton Sampler (Hydro-Bios Midi type, square aperture surface of 0.25 m²,
33 HYDRO-BIOS Apparatebau GmbH) towed horizontally at the depth of the CML at a constant
34 speed of around 2 knots (see sampling depth for each station in **Table 1**), with five
35 successive shut-off nets of 60 µm mesh-size, each of them filtering a water volume of around
36 50 to 80 m³ (estimated by automatic detection with internal and external flowmeters, and
37 according to plankton load before clogging). The analysis of zooplankton and MPs at the CML
38 was done from aliquots of samples taken with these net tows, and then fractionated by
39 sieving on board in a dedicated container under clean conditions (fractions 60-200; 200-500;
40 500-1000; 1000-2000 and > 2000 µm). All fractions were treated for zooplankton studies
41 (see Fierro-González et al., 2023). Fractions above 500 µm and the fraction 300-500 µm,
42 from the zooplankton sample 200-500 µm sieved on 300 µm mesh, were fully examined
43
44
45
46
47
48
49
50
51
52
53
54
55
56
57
58
59
60
61
62
63
64
65

1 under a binocular microscope for MPs. We separated the sample in aliquots of small
2 quantities of plankton in Dolfus chambers, then separated all the aggregates as far as
3 possible using forceps. The small number of stations (10) meant that all samples could be
4 exhaustively and meticulously observed, even though this was time-consuming.
5
6
7
8
9

10 In addition, a Manta net (opening 60 cm x 20 cm, mesh size 300 μm) was towed at the surface
11 for 20 min at 2 knots to sample an area of about 1.000 m^2 , for counting and measuring of MPs
12 following the IFREMER / MSFD - Marine Strategy Framework Directive - protocol (Hanke et al.,
13 2013). The sample from station 3 was lost. For comparison with microplastic concentrations
14 at the CML, surface MPs counts per m^2 were transformed into concentration per m^3 by
15 multiplying by 0.1 based on sampling a layer 10 cm below the surface. The relative sampling
16 efficiency of the two different sampling gears (Manta net with 300 μm mesh for surface layer
17 sampling and 60 μm mesh Multinet for horizontal CML sampling) for MPs categories and size
18 classes is discussed in Supplementary Material 1. The use of the Hydrobios midi net and Manta
19 net is nowadays the best combination of nets for sampling horizontally the surface layer and
20 oceanic layers in the water mass with accurate depth position, and with fairly comparable
21 filtered volumes (several tens of m^3).
22
23
24
25
26
27
28
29
30
31
32
33
34
35
36
37
38
39
40
41

42 Zooplankton surface counts were obtained from another Manta net with a 60 μm mesh-size
43 net, towed at a constant speed of 2 knots for 10 min, and the sieved-fractions above 200 μm
44 of this sample were used for determining MPs/zooplankton ratio at the surface. Zooplankton
45 analysis for multinet Hydrobios and Manta nets are fully described in Fierro-González et al.
46 (2023).
47
48
49
50
51
52
53

54 The quality of MPs observations was based on (members of the consortium's skills as plankton
55 observers and as microplastics specialists. Compact microplastics (pellets, films, fragments) are easily
56
57
58
59
60
61
62
63
64
65

1 recognizable, with shapes and angles that are not found in plankton organisms. Fibers can be more
2 confusing but experienced zooplankton observers can easily differentiate elongated body parts from
3
4 MPs fibers (for instance segmentation and setae of copepod antennules, used in taxonomy). Because
5
6 no chemical treatment was used in this study, the term 'fiber' is used here according to this broader
7
8 definition and it is possible that not all fibers are made from plastic. A plate with examples of photos
9
10 taken with a binocular magnifying glass to identify and measure microplastics in plankton samples
11
12 collected at the CML is presented in Supplementary Material 2. In the laboratory, these various stages
13
14 of treatments were carried out in a closed laboratory used exclusively for these observations and
15
16 following the handling recommendations to avoid sample contamination (Brander et al., 2020).
17
18
19
20

21 **Measuring MPs dimensions.** MPs collected with the 300 μm mesh-size Manta net were sieved
22
23 and sorted by size class, with four classes for the MPs (300 μm -1 mm, 1-2 mm, 2-5 mm, > 5
24
25 mm). For each size class, MPs were counted, and their typology determined (fragment, pellet,
26
27 filament/fiber, foam (mainly polystyrene) and film) under a binocular microscope (Gérigny et
28
29 al., 2022). Observations dedicated to MPs for the Hydrobios net were made with a Leica M
30
31 165C binocular microscope with camera. Length and width of each MPs item were measured.
32
33
34
35
36
37
38
39
40
41
42
43
44
45
46
47
48
49
50
51
52
53
54
55
56
57
58
59
60
61
62
63
64
65

66 **Statistical analysis.** Results of MPs concentrations, frequencies in size fractions, zooplankton
67
68 /MPs ratios, detritus/MPs ratios, in the surface water and at the CML are presented as mean
69
70 values \pm standard deviation and ranges in square brackets. Differences in mean values
71
72 between regions for surface and CML layers were tested using ANOVA, after log X+1 data
73
74 transformation to obtain normality and homoscedasticity using the Kolmogorov-Smirnov and
75
76 Levene tests. This analysis was performed using Statistica v7 software. Differences in MPs size
77
78 distribution between surface and CML were compared by calculating the Fisher-Pearson
79
80 coefficient of skewness. For the spatial patterns of abundances of MPs and % of fibers in MPs,
81
82
83
84
85

1 zooplankton and detritus, and of the ratios zooplankton/MPs and detritus/MPs, a station
2 matrix was created with square-root transformed data to estimate Bray–Curtis similarity
3 distances. The similarity matrix was then ordinated using non-metric multidimensional scaling
4 (NMDS). This analysis was performed using PRIMER v7 software.
5
6
7
8
9

10 11 12 **3. Results**

13 **Figure 1** presents the distributions of MPs, zooplankton and detritus collected at the surface
14 and at the CML, together with temperature, fluorescence and salinity profiles for the
15 different stations. Concentrations of MPs, zooplankton and detritus are presented in Log10,
16 with MPs x100 for easy comparison. In total, for the surface Manta samples, 1184 MPs items
17 (for 9 stations) were counted and classed in 4 size fractions, and for those of the Hydrobios
18 at the CML, 3165 MPs items were found and identified at all 10 stations, and for 3 of the
19 stations size measurements were made for 1317 MPs and then distributed in the same 4 size
20 fractions (**Figure 2**). At the CML, MPs abundance ranged from 10.1 to 117.9 MPs m⁻³ across
21 the 10 stations, whereas in the top 10 cm of the sea surface the range was from 0.1 to 3.4
22 MPs m⁻³ (**Table 1**). MPs at the CML were on average 96 ± 4 % fibers, the rest being either
23 fragments or films (**Figure 2 top**). In comparison, MPs found in the surface water at these
24 stations were largely dominated by fragments (89 ± 7 %). At the 3 stations where
25 comprehensive size measurements of all MPs were made for CML samples (mostly fibers),
26 the size distributions presented a similar shape declining in proportion with increasing size
27 classes (on average, 40 %, 35 %, 22 %, 3 % in classes 0.3-1, 1-2, 2-5, 5-200mm, respectively).
28 In contrast, the size distributions of the MPs collected at the surface showed variable
29 proportions in size classes (**Figure 2 bottom**). Fisher-Pearson coefficient of skewness was on
30
31
32
33
34
35
36
37
38
39
40
41
42
43
44
45
46
47
48
49
50
51
52
53
54
55
56
57
58
59
60
61
62
63
64
65

1 average 0.52 (\pm 0.12) for the distribution at the CML, and 0.29 (\pm 0.29) for the distributions
2 at the surface.
3

4
5 The microplastics concentrations and the ratios zooplankton/MPs and zooplankton/detritus
6 in the two sampled layers and visited regions showed some clear aspects (Table 1). In the
7 surface water, MPs concentrations were found in the order of 10^{-1} to 10^0 , but with no
8 significant differences between regions. Zooplankton/MPs and detritus/MPs ratio were in
9 the order of 10^2 to 10^5 . At the CML, MPs concentrations were found in the order of 10^1 to
10 10^2 , whereas zooplankton/MPs and detritus/MPs ratio were in the order of 10^0 to 10^3 . For
11
12
13
14
15
16
17
18
19
20
21
22
23
24
25
26
27
28
29
30
31
32
33
34
35
36
37
38
39
40
41
42
43
44
45
46
47
48
49
50
51
52
53
54
55
56
57
58
59
60
61
62
63
64
65

MPs concentrations at the CML, significantly lower values were found at the 3 deep sea stations compared to coastal stations ($p=0.03$).

The Non-Metric Multi-Dimensional scaling (NMDS) (**Figure 3**) provides a very good visualization of the similarities and differences between surface and CML sampling for the different stations, in relation with detritus, zooplankton and MPs contents, fibers percentage, and detritus/MPs and zooplankton/MPs ratios. Samples from the CML and surface layers are clearly distinct for all stations, in relation to the MPs content / fibers percentage axis. Secondly, while the samples from the CML tend to be grouped by zones with the exception of St.15, the samples from the surface stations are very scattered, even within same zones: this can probably be explained by the effect of differences in the conditions of the surface patchiness on MPs under the effect of high-frequency forcing (winds, surface currents).

Samples from the CML are dependent on the water column dynamics. For these samples, there is (1) a strong clustering of offshore oceanic stations (St.9, St.10, St.11) with similar MPs loads, and slight differences in mesozooplankton concentrations (as shown in Fig.1 and Table 1), (2) a clustering of NC and SC coastal stations with higher MPs loads (St.1, St.2, St.3, St.4,

1 St.17, St.19), except for St.15 whose load is more comparable to that of the offshore oceanic
2 stations. Among the coastal stations, stations 4, 17 and 19, all very shallow (< 60 m) and
3
4
5 sampled close to the bottom, form a very similar group because of their load of detritus and
6
7 zooplankton.
8
9

10 11 12 13 14 **4. Discussion** 15

16
17 During MERITE-HIPPOCAMPE, MPs were found at all stations both at the surface and at the
18
19 CML. The observation of MPs at the surface is widely documented and is now carried out in
20
21 accordance with standards (Hanke et al., 2013). In the Mediterranean, it is estimated that
22
23 MPs are found over almost all the sea-surface (Collignon et al., 2012; Fabri-Ruiz et al., 2023).
24
25 Our observed MPs surface concentrations did not show identifiable regional differences due
26
27 to high variability between stations, related to the characteristics of local transport (Rwawi
28
29 et al. 2023). The surface MPs quantified during our campaign with the 300 µm mesh-size
30
31 Manta net (0.005 to 0.343 MPs m⁻²) are within the classical range of observations in the
32
33 Mediterranean as presented in the review by Cincinelli et al. (2019).
34
35
36
37
38
39
40

41 On the other hand, MPs observations in the water column are much less numerous, and also
42
43 much less standardized in terms of protocols. They are either obtained by vertical net tows
44
45 for zooplankton (e.g., Lefebvre et al., 2019), or by using bottles that can be closed at the
46
47 desired depths but with a limited volume (e.g., Tamminga et al., 2018; Dai et al., 2018), or by
48
49 sediment traps for long-term observation of sinking MPs (e.g., Galgani et al., 2022).
50
51

52 Collection of MPs by pumping is restricted to sub-surface samples in the upper 15 m (see
53
54 Table 2 in Montoto-Martinez et al., 2020). The use of a Hydrobios Midi Multinet for MPs has
55
56
57
58
59 been done before, but for closing net vertical tows (Zhao et al., 2022, with 100 µm mesh-size
60
61
62
63
64
65

1 nets), but its use for perfectly horizontal tows with a layer thickness of 0.25 m within the
2 densest in situ plankton layers, as in our study, is, to our knowledge, new. Our observations
3 of MPs concentrations at the CML (with 60 μm mesh nets; fraction > 200 μm) varied
4 between 10 and 120 MPs m^{-3} at the level of these dense planktonic layers. The rare
5 publications providing concentrations in the water column give very variable values
6 depending on the sampling device. With a 90 μm mesh-size closing net, Gorokhova (2015)
7 found that intermediate layers (30-60 m) in the 100 m deep water column have more MPs
8 per unit volume than upper (0-30 m) or deeper (60-100 m) layers, and reach 10^2 - 10^4 MPs m^{-3}
9 in this intermediate layer. Similarly, Uurasjärvi et al. (2021) using both closing nets with a
10 100 μm mesh-size towed vertically in the intermediate layers and 30 L volume closing bottles
11 found variations of 10^0 - 10^3 MPs m^{-3} . Choy et al (2019) present a distribution of MPs over the
12 whole water column in the deep-sea area of Monterey Bay (from surface to 1000 m)
13 sampling with a ROV (their Fig1). The distribution suggests a first local maximum of MPs
14 below the surface at 25 m (which corresponds to the local *Chla* maximum layer, see Monterey
15 Bay Time Series Data, <https://www.mbari.org/data/mbts-data/>) followed by a decrease down to
16 75 m, and then a rapid increase below this depth down to the bottom of the mixed layer
17 (around 200 m), to slowly decrease again downwards. They specify that most of these MPs
18 are fibers (see their Figure S4 in their online supplementary and the associated legend text
19 information - <https://doi.org/10.1038/s41598-019-44117-2>), and they are in the same order of
20 magnitude as those we observed.

21 Our MPs results are rare because they were obtained for large volumes in thin horizontal
22 layers at the level of the CML using the Hydrobios net, and they show that the densities of
23 MPs observed in this CML layer are higher than those at the surface, and that this pattern is
24 more marked in coastal areas than in offshore areas. It is likely that in coastal areas,

1 resuspension of suprabenthic detritus including MPs can maintain a relatively high particle
2 load in the intermediate layers (Chevalier et al., 2023), whereas at offshore ocean stations,
3
4 the observed concentrations of MPs at the CML are not greatly affected by vertical
5
6 resuspension, and certainly not from the benthic reservoir.
7
8

9
10 The very high proportion of fibers distributed in all size classes (based on their length)
11
12 (Figure 2) is probably partly linked to the mesh size of our nets and our vertical sampling
13
14 protocol in the densest planktonic layers, which inevitably leads to clogging. Larger mesh
15
16 sizes and towed nets avoiding clogging are clearly not suitable for collecting fibers.
17
18

19
20 Conversely, closing bottles are probably the best sampling tool for this. Dai et al. (2018),
21
22 when studying the fine vertical distribution of MPs in the water column of Bohai Bay using
23
24 10 L Niskin bottles, detected fiber proportions of 75 % to 96.4 % of the total MPs, with
25
26 accumulation in the intermediate layers. The distribution of fiber sizes in the few samples
27
28 where these measurements have been made (Figure 2) deserves further investigation: the
29
30 relative regularity of these fiber size distributions at the CML may be related to mechanical
31
32 or biological phenomena of fiber fractionation.
33
34
35
36

37
38 Fibers, films and fragments from CML samples have often been observed under a binocular
39
40 loupe to be trapped in an organic matrix (marine snow, aggregates). This may be due to
41
42 aggregate-microplastic complexes formed *in situ* but may also be enhanced by the sample
43
44 collection and sieving protocol. However, the fate and transport of MPs has previously been
45
46 reported to be intrinsically linked to marine snow formation (Möller et al., 2012; Porter et
47
48 al., 2018; Kvale et al., 2020), but the resulting aggregate-MPs complexes have instead been
49
50 mostly considered as a factor increasing the vertical transport of MPs to the seabed and
51
52 potentially impacting the benthos (Porter et al., 2018; Kvale et al., 2020). For MPs having a
53
54 density close to the water density, such as polypropylene fibers, it is possible that they are
55
56
57
58
59
60
61
62
63
64
65

1 trapped and accumulated in thin layers of perennial marine snow (Zhao et al., 2022)
2 promoting denser layers of fibers, which accumulate and float over a long period (Prairie et
3 al., 2015). Our observations even suggest that the fibers become micro-skeletons of marine
4 snow or aggregates. Nevertheless, it is also possible that the larger fibers structure larger
5 aggregates of marine snow which ultimately trap other particles which increase
6 sedimentation. Fiber size distributions at the CML may be a consequence of differences in
7 the stability of aggregate-MP complexes at density interfaces.
8
9

10 The zooplankton/microplastic ratio is considered a valid index of the impact of MPs on
11 planktonic biota (Gerigny et al., 2022), and can be used to characterize a potential impact of
12 microplastics loading on the prey available to planktivorous fish (Fabri-Ruiz et al., 2023).
13
14

15 However, it can be seen that these ratios obtained during the Hippocampe cruise are
16 extremely variable from one station to another (Table 1), for both the surface and CML
17 layers. An in-depth analysis of the relative vertical distributions of zooplankton and
18 microplastics would require taking into account, at each station, the recent dynamic history
19 of the water masses in the epipelagic layer and the dynamics of the water column (over a
20 few days), which have a very strong influence on the establishment of physical gradients in
21 the water column and therefore of chemical and biotic gradients (Rwawy et al., 2023;
22 Chevalier et al., 2023). All the features are also highlighted by the NMDS analysis.
23
24

25 Our observations show that detritus and phytoplankton aggregates are always more
26 abundant in the CML than in the surface layer, which is also the case for microplastics
27 (Figure 1), mainly of the fiber type (Figure 2). It is well recognized that thin layers of
28 phytoplankton and marine snow particles are associated with strong density gradients
29 inducing reduced fall rates (Alldredge et al., 2002), so it is hardly surprising to find here
30 higher proportion of buoyant microplastics.
31
32
33
34
35
36
37
38
39
40
41
42
43
44
45
46
47
48
49
50
51
52
53
54
55
56
57
58
59
60
61
62
63
64
65

1 Fierro-Gonzalez et al. (2023) analyze in detail the observed differences in stocks of
2 zooplankton, detritus and microphytoplankton aggregates and in the relative distributions of
3 zooplankton taxonomic groups at the level of the surface and CML layers (see their Fig. 4),
4 and over the whole water column (0-200 m, or 0-bottom for stations with bathymetry < 200
5 m). In general, the surface layer is distinguished from the rest of the water column by
6 relatively stronger representations of certain taxa (copepods, crustaceans or gelatinous
7 plankton) with species that are often characteristic of the hyponeuston, and which can
8 proliferate there (Champalbert, 1971).
9

10 At the CML layer, the general pattern over the Hippocampe cruise highlights specific
11 features in the distribution of taxonomic groups compared with the average concentrations
12 in the water column: greater proportions of copepods, nauplii, and other crustaceans, much
13 smaller proportions of herbivorous gelatinous plankton (appendicularians, salps) and
14 pteropods, and carnivorous plankton (chaetognaths, jellyfish). Recent studies using cameras
15 allowing a fine vertical resolution, either towed on a platform (Möller et al., 2012; Greer et
16 al., 2020) or placed on a glider (Whitemore and Ohman, 2021), show similar patterns of
17 different relative distributions of taxonomic groups between dense layers of fine particles
18 and the rest of the epipelagic water column.
19

20 Studies of the distribution and behaviour of mesozooplanktonic organisms show that certain
21 groups tend to aggregate in these fine layers, while others seek to avoid them (Greer et al.
22 2013). Zooplankton taxa that are strict phytoplankton filter feeders, either with appendages
23 or with filtering systems, tend to avoid layers with high densities of detrital particles that
24 obstruct their filtering systems (appendicularians, salps, some of calanoid copepods) and will
25 feed on phytoplankton and particles in more diluted layers. Inversely, many omnivorous
26 filter- feeders and ambush feeders, either omnivorous-herbivorous (most calanoid
27
28
29
30
31
32
33
34
35
36
37
38
39
40
41
42
43
44
45
46
47
48
49
50
51
52
53
54
55
56
57
58
59
60
61
62
63
64
65

1 copepods), or omnivorous-carnivorous Cyclopoida and Poecilostomatoida (i.e. Oithonidae,
2 Oncaeidae and Corycaeidae), or omnivorous-detritivorous (harpacticoids), tend to aggregate
3
4 in dense layers (Möller et al., 2012; Koski et al., 2017) associated with bacterial and microbial
5 development (Kiorboe, 2001). In addition, other planktonic crustaceans (larvae and juveniles
6
7 of mysids, ostacods and amphipods) also consume particles and microzooplankton that are
8
9 colonizing marine snow aggregates (see quoted papers in Möller et al., 2012).

10 These zooplankton taxonomic groups found in the CML are among the favorite prey of small
11
12 pelagic fish (Chen et al, 2022), that exploit dense layers of particles and zooplankton (Benoit-
13
14 Bird, 2009; Möller et al, 2012), and it is therefore important to assess the quantity and
15
16 quality of MPs in these layers that can be swallowed accidentally by fish. In their joint study
17
18 of MPs concentrations in the water column and the stomach contents of fish in the Gulf of
19
20 Lion, Lefebvre et al. (2019) showed a relatively low occurrence of MPs in fish stomachs
21
22 (around 10% of individuals), and fibers were the only type of MPs encountered in the
23
24 digestive tracts. Their results are consistent with the relatively high ratio zooplankton/MPs
25
26 (> 10⁴ in our study) in the dense layers (CML for us) preyed on by planktivorous fish.
27
28

29 In our results, the lowest zooplankton/microplastics ratios were obtained for stations in
30
31 outer continental shelf zones (St. 3 and St. 15) or in oceanic zones close to the slope (St. 2
32
33 and St. 11), while the highest ratios were obtained for either inshore littoral zones (St. 1, St.
34
35 4, St. 17, St. 19) or offshore oceanic zones (St. 9 and St. 10). Espinasse et al. (2014), in their
36
37 study of particle and zooplankton distributions in the Gulf of Lion, showed that beyond the
38
39 100 m isobath from the continental shelf to the oceanic waters above the shelf break, the
40
41 zooplankton is aggregated in very dense layers located between 20 and 40 m, whereas in the
42
43 area close to the coast (below the 100m isobath), the water mass is strongly stirred with
44
45 homogenized distributions of particles and zooplankton throughout the water column. This
46
47
48
49
50
51
52
53
54
55
56
57
58
59
60
61
62
63
64
65

1 suggests that further studies on the associated distributions of microplastics and
2 zooplankton should take into account knowledge of the structuring of planktonic habitats, as
3 done for example by Espinasse et al (2014), and characterize the MPs/zooplankton ratios in
4 key layers of the water column, not only at the surface.
5
6
7
8
9

10 11 12 **5. Concluding remarks**

13 Two major interfaces promote the accumulation of MPs: the air-sea surface interface with
14 the accumulation of MPs less dense than seawater, and the water-sediment interface where
15 MPs denser than seawater accumulate. Our observations based on horizontal sampling with
16 a Multinet Hydrobios midi in the densest planktonic layers of the water column, close to the
17 chlorophyll maximum, highlight a high concentration of MPs mainly fibers (sometimes films
18 and fragments) associated with high levels of detrital aggregates. Although our protocol may
19 have amplified these MPs-aggregate complexes, our results enable us to propose that sub-
20 surface dense layers of marine snow and plankton represent a third major marine interface
21 for MPs types with a density close to that of water and floating in the water column and will
22 have to be considered in future MPs distribution modeling efforts. Clearly, the use of
23 Multinet nets allowing targeting of particular layers associated with dedicated bottle
24 sampling represents a suitable methodological approach to better characterize the MPs load
25 of these productive oceanic layers. This is all the more important as the major trophic
26 interaction layers between zooplankton and their prey and between fish and their
27 zooplankton prey are mainly these dense layers.
28
29
30
31
32
33
34
35
36
37
38
39
40
41
42
43
44
45
46
47
48
49
50
51
52
53
54
55
56
57
58
59
60
61
62
63
64
65

Acknowledgements

1
2
3 This work was supported by the French National program EC2CO (Ecosphère Continentale et
4
5 Côtière) with funding from the project Pelagoplastics (#°13082 Call EC2CO2020; PI: F. Carlotti).
6

7
8 The MERITE-HIPPOCAMPE project has been funded by the cross-disciplinary Pollution &
9
10 Contaminants axis of the CNRS-INSU MISTRALS program (joint action of the MERMEX-MERITE
11
12 and CHARMEX subprograms) and received support from the IRD French-Tunisian International
13
14 Joint Laboratory (LMI) COSYS-Med. We are grateful to the captains and crew of the R/V Antea
15
16 for their help and assistance during the cruise, as well as the scientific crew for help in
17
18 collecting and processing net samples on board. Zooplankton and microplastics analyses were
19
20 carried out on the Microscopy and Imaging platform of MIO, which is partly funded by the
21
22 European FEDER Fund (project no. 1166-39417). Our thanks to all the participants involved in
23
24 the MERITE HIPPOCAMPE project. Special thanks to Marc Tedetti for his continuous support
25
26 and his critical review of the paper. Thanks are also addressed to Michael Paul, native speaker,
27
28 for English proofreading. Pamela Fierro González was supported by a Becas-Chile N°72190675
29
30 PhD scholarship by the National Agency for Research and Development (ANID), Government
31
32 of Chile. Javier Tesán-Onrubia was supported by the CONTAMPUMP project (ANR JCJC #19-
33
34 CE34-0001-01). We also acknowledge the contributions of the reviewers for their constructive
35
36 comments and suggestions.
37
38
39
40
41
42
43
44
45
46
47
48
49
50
51
52
53
54
55
56
57
58
59
60
61
62
63
64
65

References

- 1
2
3 Alldredge, A. L., Cowles T. J., MacIntyre S., JRines. E. B., Donaghay P. L., Greenlaw C. F., and
4
5 Zaneveld J. R. V.. 2002. O2002. Occurrence and mechanisms of formation of a dramatic
6
7 thin layer of marine snow in a shallow Pacific fjord. *Mar. Ecol. Prog. Ser.* 233: 1–12.
8
9
10 doi:10.3354/meps233001
11
12
13
14 Alldredge, A.L., Silver, M.W., 1988. Characteristics, dynamics and significance of marine
15
16 snow. *Progress in Oceanography* 20, 41-82. [https://doi.org/10.1016/0079-6611\(88\)90053-5](https://doi.org/10.1016/0079-6611(88)90053-5)
17
18
19
20 Benoit-Bird, K.J., 2009. Dynamic 3-dimensional structure of thin zooplankton layers is
21
22 impacted by foraging fish. *Marine Ecology Progress Series*, 396, 61–76.
23
24
25 <https://doi.org/10.3354/meps08316>
26
27
28
29 Brander, S.M., Renick, V.C., Foley, M.M., Steele, C., Woo, M., Lusher, A., Carr, S., Helm, P.,
30
31 Box, C., Cherniak, S., Andrews, R.C., Rochman, C.M., 2020. Sampling and quality assurance
32
33 and quality control: a guide for scientists investigating the occurrence of microplastics
34
35 across matrices. *Appl. Spectrosc.* 74 (9), 1099–1125.
36
37
38
39 <https://doi.org/10.1177/0003702820945713>
40
41
42
43 Champalbert, G., 1971. Variations nyctémérales du plancton superficiel. II. Espèces non
44
45 caractéristique de l'hyponeuston et hyponeuston nocturne. *Journal of Experimental*
46
47 *Marine Biology and Ecology* 6, 55-70.
48
49
50
51 Chen, C., Carlotti, F., Harmelin-Vivien, M., Lebreton, B., Guilloux, G., Vassallo, L., Le Bihan,
52
53 M., Bănaru, D., 2022. Diet and trophic interactions of Mediterranean planktivorous fishes.
54
55 *Marine Biology*, 169. <https://doi.org/10.1007/s00227-022-04103-1>
56
57
58
59
60
61
62
63
64
65

- 1 Chevalier, C., Vandenberghe, M., Pagano, M., Pellet, I., Pinazo, C., Tesán Onrubia, J.A.,
2
3 Guilloux, L., Carlotti, F., 2023. Investigation of dynamic change in microplastics vertical
4
5 distribution patterns: The seasonal effect on vertical distribution. *Marine Pollution*
6
7 *Bulletin*, 189, 114674. <https://doi.org/10.1016/j.marpolbul.2023.114674>
8
9
- 10 Choy, C.A., Robison, B.H., Gagne, T.O., Erwin, B., Firl, E., Halden, R.U., Hamilton, J.A., Katija,
11
12 K., Lisin, S.E., Rolsky, C., 2019. The vertical distribution and biological transport of marine
13
14 microplastics across the epipelagic and mesopelagic water column. *Scientific Reports* 9,
15
16 7843. DOI: [10.1038/s41598-019-44117-2](https://doi.org/10.1038/s41598-019-44117-2)
17
18
19
- 20 Cincinelli, A., Martellini, T., Guerranti, C., Scopetani, C., Chelazzi, D., Giarrizzo, T., 2019. A
21
22 potpourri of microplastics in the sea surface and water column of the Mediterranean Sea.
23
24 *Trends in Analytical Chemistry*, 110, 321–326. <https://doi.org/10.1016/j.trac.2018.10.026>
25
26
27
- 28 Cole, M., Lindeque, P., Halsband, C., Galloway, T.S., 2011 Microplastics as contaminants in
29
30 the marine environment: A review. *Mar. Marine Pollution Bulletin*, 62:2588–2597
31
32
33 <https://doi.org/10.1016/j.marpolbul.2011.09.025>
34
35
36
- 37 Collignon, A., Hecq, J.-H., Galgani, F., Voisin, P., Collard, F., Goffart, A., 2012. Neustonic
38
39 microplastic and zooplankton in the North Western Mediterranean Sea. *Marine Pollution*
40
41 *Bulletin* 64, 861–864. <https://doi.org/10.1016/j.marpolbul.2012.01.011>
42
43
44
- 45 Dai, Z., Zhang, H., Zhou, Q., Tian, Y., Chen, T., Tu, C., Fu, C., Luo, Y., 2018. Occurrence of
46
47 microplastics in the water column and sediment in an inland sea affected by intensive
48
49 anthropogenic activities. *Environmental Pollution*, 242, 1557–1565
50
51
52
53
54
55 <https://doi.org/10.1016/j.envpol.2018.07.131>
56
57
58
59
60
61
62
63
64
65

1
2
3
4
5
6
7
8
9
10
11
12
13
14
15
16
17
18
19
20
21
22
23
24
25
26
27
28
29
30
31
32
33
34
35
36
37
38
39
40
41
42
43
44
45
46
47
48
49
50
51
52
53
54
55
56
57
58
59
60
61
62
63
64
65

Espinasse, B., Carlotti, F., Zhou, M., Devenon, J.L., 2014. Defining zooplankton habitats in the Gulf of Lion (NW Mediterranean Sea) using size structure and environmental conditions.

Marine Ecology Progress Series 506, 31-46. DOI: 10.3354/meps10803

Fabri-Ruiz, S., Baudena, A., Moullec, F., Lombard, F., Irisson, J.-O., Pedrotti, M.L., 2023.

Mistaking plastic for zooplankton: Risk assessment of plastic ingestion in the Mediterranean Sea. *Science of the Total Environment*, 856 (2), pp.159011.

<https://doi.org/10.1016/j.scitotenv.2022.159011>

Fierro-González, P., Pagano, M., Guilloux, L., Makhlof Belkahia, N., Tedetti, M., Carlotti, F.,

2023. Zooplankton biomass, size structure, and associated metabolic fluxes with focus on its roles at the chlorophyll maximum layer during the plankton-contaminant MERITE-

HIPPOCAMPE cruise. *Marine Pollution Bulletin* 193 (2023) 115056

<https://doi.org/10.1016/j.marpolbul.2023.115056>

Galgani, L., Goßmann, I., Scholz-Böttcher, B., Jiang, X., Liu, Z., Scheidemann, L., Schlundt, C.,

Engel, A., 2022. Hitchhiking into the Deep: How Microplastic Particles are Exported

through the Biological Carbon Pump in the North Atlantic Ocean. *Environmental Science*

& Technology, 56(22):15638-15649. <https://doi.org/10.1021/acs.est.2c04712>

Gérigny, O., Pedrotti, M.-L., El Rakwe, M., Brun, M., Pavec, M., Henry, M., Mazeas, F., Maury,

J., Garreau, P., Galgani, F., 2022. Characterization of floating microplastic contamination

in the bay of Marseille (French Mediterranean Sea) and its impact on zooplankton and

mussels. *Marine Pollution Bulletin*, 175, 113353.

<https://doi.org/10.1016/j.marpolbul.2022.113353>

1 Gorokhova, E., 2015. Screening for microplastic particles in plankton samples: How to
2 integrate marine litter assessment into existing monitoring programs? Marine Pollution
3 Bulletin 99(1-2):271-275. <https://doi.org/10.1016/j.marpolbul.2015.07.056>
4
5
6

7
8 Greer, A. T., R. K. Cowen, C. M. Guigand, M. A. McManus, J. C. Sevadjan, and A. H. V.
9

10 Timmerman. 2013. Relationships between phytoplankton thin layers and the finescale
11 vertical distributions of two trophic levels of zooplankton. J. Plankton Res. 35: 939–956.
12
13
14
15
16 doi:10.1093/ plankt/fbt056
17 Greer et al., 2020

18
19 Greer, A.T., A.D. Boyette, V.J. Cruz, M.K. Cambazoglu, B. Dzwonkowski, L.M. Chiaverano, S.L.
20

21 Dykstra, C. Briseño-Avena, R.K. Cowen, and J.D. Wiggert. 2020. Contrasting fine-scale
22 distributional patterns of zooplankton driven by the formation of a diatom-dominated
23
24
25
26
27
28
29 thin layer. Limnology & Oceanography 65(9):2236-2258. doi: 10.1002/lno.11450

30 Hanke, G., Galgani, F., Werner, S., Oosterbaan, L., Nilsson, P., Fleet, D., Kinsey, S., Thompson,
31

32 R.C., Van Franeker, J., Vlachogianni, T., Scoullou, M., Veiga, J.M., Palatinus, A., Matiddi,
33

34 M., Maes, T., Korpinen, S., Budziak, A., Leslie, H., Gago, J., Liebezeit, G., 2013. Guidance on
35
36
37
38
39
40
41
42 Monitoring of Marine Litter in European Seas: a guidance document within the Common
43
44
45
46
47
48
49
50
51
52
53
54
55
56
57
58
59
60
61
62
63
64
65
66
67
68
69
70
71
72
73
74
75
76
77
78
79
80
81
82
83
84
85
86
87
88
89
90
91
92
93
94
95
96
97
98
99
100
101
102
103
104
105
106
107
108
109
110
111
112
113
114
115
116
117
118
119
120
121
122
123
124
125
126
127
128
129
130
131
132
133
134
135
136
137
138
139
140
141
142
143
144
145
146
147
148
149
150
151
152
153
154
155
156
157
158
159
160
161
162
163
164
165
166
167
168
169
170
171
172
173
174
175
176
177
178
179
180
181
182
183
184
185
186
187
188
189
190
191
192
193
194
195
196
197
198
199
200
201
202
203
204
205
206
207
208
209
210
211
212
213
214
215
216
217
218
219
220
221
222
223
224
225
226
227
228
229
230
231
232
233
234
235
236
237
238
239
240
241
242
243
244
245
246
247
248
249
250
251
252
253
254
255
256
257
258
259
260
261
262
263
264
265
266
267
268
269
270
271
272
273
274
275
276
277
278
279
280
281
282
283
284
285
286
287
288
289
290
291
292
293
294
295
296
297
298
299
300
301
302
303
304
305
306
307
308
309
310
311
312
313
314
315
316
317
318
319
320
321
322
323
324
325
326
327
328
329
330
331
332
333
334
335
336
337
338
339
340
341
342
343
344
345
346
347
348
349
350
351
352
353
354
355
356
357
358
359
360
361
362
363
364
365
366
367
368
369
370
371
372
373
374
375
376
377
378
379
380
381
382
383
384
385
386
387
388
389
390
391
392
393
394
395
396
397
398
399
400
401
402
403
404
405
406
407
408
409
410
411
412
413
414
415
416
417
418
419
420
421
422
423
424
425
426
427
428
429
430
431
432
433
434
435
436
437
438
439
440
441
442
443
444
445
446
447
448
449
450
451
452
453
454
455
456
457
458
459
460
461
462
463
464
465
466
467
468
469
470
471
472
473
474
475
476
477
478
479
480
481
482
483
484
485
486
487
488
489
490
491
492
493
494
495
496
497
498
499
500
501
502
503
504
505
506
507
508
509
510
511
512
513
514
515
516
517
518
519
520
521
522
523
524
525
526
527
528
529
530
531
532
533
534
535
536
537
538
539
540
541
542
543
544
545
546
547
548
549
550
551
552
553
554
555
556
557
558
559
560
561
562
563
564
565
566
567
568
569
570
571
572
573
574
575
576
577
578
579
580
581
582
583
584
585
586
587
588
589
590
591
592
593
594
595
596
597
598
599
600
601
602
603
604
605
606
607
608
609
610
611
612
613
614
615
616
617
618
619
620
621
622
623
624
625
626
627
628
629
630
631
632
633
634
635
636
637
638
639
640
641
642
643
644
645
646
647
648
649
650
651
652
653
654
655
656
657
658
659
660
661
662
663
664
665
666
667
668
669
670
671
672
673
674
675
676
677
678
679
680
681
682
683
684
685
686
687
688
689
690
691
692
693
694
695
696
697
698
699
700
701
702
703
704
705
706
707
708
709
710
711
712
713
714
715
716
717
718
719
720
721
722
723
724
725
726
727
728
729
730
731
732
733
734
735
736
737
738
739
740
741
742
743
744
745
746
747
748
749
750
751
752
753
754
755
756
757
758
759
760
761
762
763
764
765
766
767
768
769
770
771
772
773
774
775
776
777
778
779
780
781
782
783
784
785
786
787
788
789
790
791
792
793
794
795
796
797
798
799
800
801
802
803
804
805
806
807
808
809
810
811
812
813
814
815
816
817
818
819
820
821
822
823
824
825
826
827
828
829
830
831
832
833
834
835
836
837
838
839
840
841
842
843
844
845
846
847
848
849
850
851
852
853
854
855
856
857
858
859
860
861
862
863
864
865
866
867
868
869
870
871
872
873
874
875
876
877
878
879
880
881
882
883
884
885
886
887
888
889
890
891
892
893
894
895
896
897
898
899
900
901
902
903
904
905
906
907
908
909
910
911
912
913
914
915
916
917
918
919
920
921
922
923
924
925
926
927
928
929
930
931
932
933
934
935
936
937
938
939
940
941
942
943
944
945
946
947
948
949
950
951
952
953
954
955
956
957
958
959
960
961
962
963
964
965
966
967
968
969
970
971
972
973
974
975
976
977
978
979
980
981
982
983
984
985
986
987
988
989
990
991
992
993
994
995
996
997
998
999
1000

European Commission, Joint Research Centre, 128pp. <https://doi.org/10.2788/99475>

46 Kiørboe T (2001) Formation and fate of marine snow: small scale processes with large-scale
47 implications. Sci Mar 65(Suppl): 57–71 DOI: 10.3989/scimar.2001.65s257
48
49
50

51
52 Koski M, Boutorh J, de la Rocha C (2017). Feeding on dispersed vs. aggregated particles: The
53 effect of zooplankton feeding behavior on vertical flux. PLoS ONE 12(5): e0177958.
54
55
56
57
58
59
60
61
62
63
64
65
66
67
68
69
70
71
72
73
74
75
76
77
78
79
80
81
82
83
84
85
86
87
88
89
90
91
92
93
94
95
96
97
98
99
100
101
102
103
104
105
106
107
108
109
110
111
112
113
114
115
116
117
118
119
120
121
122
123
124
125
126
127
128
129
130
131
132
133
134
135
136
137
138
139
140
141
142
143
144
145
146
147
148
149
150
151
152
153
154
155
156
157
158
159
160
161
162
163
164
165
166
167
168
169
170
171
172
173
174
175
176
177
178
179
180
181
182
183
184
185
186
187
188
189
190
191
192
193
194
195
196
197
198
199
200
201
202
203
204
205
206
207
208
209
210
211
212
213
214
215
216
217
218
219
220
221
222
223
224
225
226
227
228
229
230
231
232
233
234
235
236
237
238
239
240
241
242
243
244
245
246
247
248
249
250
251
252
253
254
255
256
257
258
259
260
261
262
263
264
265
266
267
268
269
270
271
272
273
274
275
276
277
278
279
280
281
282
283
284
285
286
287
288
289
290
291
292
293
294
295
296
297
298
299
300
301
302
303
304
305
306
307
308
309
310
311
312
313
314
315
316
317
318
319
320
321
322
323
324
325
326
327
328
329
330
331
332
333
334
335
336
337
338
339
340
341
342
343
344
345
346
347
348
349
350
351
352
353
354
355
356
357
358
359
360
361
362
363
364
365
366
367
368
369
370
371
372
373
374
375
376
377
378
379
380
381
382
383
384
385
386
387
388
389
390
391
392
393
394
395
396
397
398
399
400
401
402
403
404
405
406
407
408
409
410
411
412
413
414
415
416
417
418
419
420
421
422
423
424
425
426
427
428
429
430
431
432
433
434
435
436
437
438
439
440
441
442
443
444
445
446
447
448
449
450
451
452
453
454
455
456
457
458
459
460
461
462
463
464
465
466
467
468
469
470
471
472
473
474
475
476
477
478
479
480
481
482
483
484
485
486
487
488
489
490
491
492
493
494
495
496
497
498
499
500
501
502
503
504
505
506
507
508
509
510
511
512
513
514
515
516
517
518
519
520
521
522
523
524
525
526
527
528
529
530
531
532
533
534
535
536
537
538
539
540
541
542
543
544
545
546
547
548
549
550
551
552
553
554
555
556
557
558
559
560
561
562
563
564
565
566
567
568
569
570
571
572
573
574
575
576
577
578
579
580
581
582
583
584
585
586
587
588
589
590
591
592
593
594
595
596
597
598
599
600
601
602
603
604
605
606
607
608
609
610
611
612
613
614
615
616
617
618
619
620
621
622
623
624
625
626
627
628
629
630
631
632
633
634
635
636
637
638
639
640
641
642
643
644
645
646
647
648
649
650
651
652
653
654
655
656
657
658
659
660
661
662
663
664
665
666
667
668
669
670
671
672
673
674
675
676
677
678
679
680
681
682
683
684
685
686
687
688
689
690
691
692
693
694
695
696
697
698
699
700
701
702
703
704
705
706
707
708
709
710
711
712
713
714
715
716
717
718
719
720
721
722
723
724
725
726
727
728
729
730
731
732
733
734
735
736
737
738
739
740
741
742
743
744
745
746
747
748
749
750
751
752
753
754
755
756
757
758
759
760
761
762
763
764
765
766
767
768
769
770
771
772
773
774
775
776
777
778
779
780
781
782
783
784
785
786
787
788
789
790
791
792
793
794
795
796
797
798
799
800
801
802
803
804
805
806
807
808
809
810
811
812
813
814
815
816
817
818
819
820
821
822
823
824
825
826
827
828
829
830
831
832
833
834
835
836
837
838
839
840
841
842
843
844
845
846
847
848
849
850
851
852
853
854
855
856
857
858
859
860
861
862
863
864
865
866
867
868
869
870
871
872
873
874
875
876
877
878
879
880
881
882
883
884
885
886
887
888
889
890
891
892
893
894
895
896
897
898
899
900
901
902
903
904
905
906
907
908
909
910
911
912
913
914
915
916
917
918
919
920
921
922
923
924
925
926
927
928
929
930
931
932
933
934
935
936
937
938
939
940
941
942
943
944
945
946
947
948
949
950
951
952
953
954
955
956
957
958
959
960
961
962
963
964
965
966
967
968
969
970
971
972
973
974
975
976
977
978
979
980
981
982
983
984
985
986
987
988
989
990
991
992
993
994
995
996
997
998
999
1000

- 1
2
3
4
5
6
7
8
9
10
11
12
13
14
15
16
17
18
19
20
21
22
23
24
25
26
27
28
29
30
31
32
33
34
35
36
37
38
39
40
41
42
43
44
45
46
47
48
49
50
51
52
53
54
55
56
57
58
59
60
61
62
63
64
65
- Kukulka, T., Proskurowski, G., Mor'et-Ferguson, S., Meyer, D.W., Law, K.L., 2012. The effect of wind mixing on the vertical distribution of buoyant plastic debris. *Geophys. Res. Lett.* 39. DOI: 10.1029/2012GL051116
- Kvale, K.F., Prowe, A.E.F., Oschlies, A.A., 2020. A critical examination of the role of marine snow and zooplankton fecal pellets in removing ocean surface microplastic. *Frontiers in Marine Science*, 6, 808. <https://doi.org/10.3389/fmars.2019.00808>
- Lefebvre, C., Saraux, C., Heitz, O., Nowaczyk, A., Bonnet, D., 2019. Microplastics FTIR Characterisation and Distribution in the Water Column and Digestive Tracts of Small Pelagic Fish in the Gulf of Lions. *Marine Pollution Bulletin*, 142, 510-519. <https://doi.org/10.1016/j.marpolbul.2019.03.025>
- Mendrik, F., Fernández, R., Hackney, C.R. Waller C., Parsons D.R., 2023. Non-buoyant microplastic settling velocity varies with biofilm growth and ambient water salinity. *Commun Earth Environ* 4, 30. <https://doi.org/10.1038/s43247-023-00690-z>
- Möller, K.O., John, M.S., Temming, A., Floeter, J., Sell, A.F., Herrmann, J.P., Möllmann, C., 2012. Marine snow, zooplankton and thin layers: indications of a trophic link from small-scale sampling with the video plankton recorder. *Marine Ecology Progress Series*, 468, 57–69. <https://doi.org/10.3354/meps09984>
- Montoto-Martinez, T., Hernandez-Brito, J.J., Gelado-Caballero, M.D., 2020. Pump-underway ship intake: An unexploited opportunity for Marine Strategy Framework Directive (MSFD) microplastic monitoring needs on coastal and oceanic waters. *PLoS ONE* 15(5): e0232744. <https://doi.org/10.1371/journal.pone.0232744>

1 Prairie, J.C., Ziervogel, K., Camassa, R., McLaughlin, R.M., White, B.L., Dewald, C., Arnosti, C.,

2 2015. Delayed settling of marine snow: Effects of density gradient and particle properties

3 and implications for carbon cycling. *Marine Chemistry*, 175, 28–38.

4 <https://doi.org/10.1016/j.marchem.2015.04.006>

5 Porter, A., Lyons, B.P., Galloway, T.S., Lewis, C., 2018. Role of marine snows in microplastic

6 fate and bioavailability. *Environmental Science & Technology*, 52, 7111–7119.

7 <https://doi.org/10.1021/acs.est.8b01000>

8 Rwawi, C., Hernandez-Carrasco, I., Sudre, F., Tedetti, M., Rossi V., 2023. Transport patterns

9 and hydrodynamic context of the HIPPOCAMPE cruise: implications for contaminants

10 distribution and origin. *Marine Pollution Bulletin*, this issue, in revision.

11 Tamminga, M., Hengstmann, E., Fischer, E.K., 2018. Microplastic analysis in the South Funen

12 Archipelago, Baltic Sea, implementing manta trawling and bulk sampling. *Marine*

13 *Pollution Bulletin* 128, 601e608. <https://doi.org/10.1016/j.marpolbul.2018.01.066>

14 Tedetti, M., Tronczynski, J., Carlotti, F., Pagano, M., Sammari, C., Bel Hassen, M., Ben Ismail,

15 S., Desboeufs, K., Poindron, C., Chifflet, S., Abdennadher, M., Amri, S., Bănarua, D., Ben

16 Abdallah, L., Bhairy, N., Boudriga, I., Bourin, A., Brach-Papa, C., Briant, N., Cabrol, L.,

17 Chevalier, C., Chouba, L., Coudray, S., Daly Yahia, M.N., de Garidel-Thoron, T., Dufour, A.,

18 Dutay, J.-C., Espinasse, B., Fierro-González, P., Fournier, M., Garcia, N., Giner, F., Guigue, C.,

19 Guilloux, L., Hamza, A., Heimbürger-Boavida, L.-E., Jacquet, S., Knoery, J., Lajnef, R.,

20 Makhoulf Belkahia, N., Malengros, D., Martinot, P.L., Bosse, A., Mazur, J.-C., Meddeb, M.,

21 Misson, B., Pringault, O., Quéméneur, M., Radakovitch, O., Raimbault, P., Ravel, C., Rossi,

22 V., Rwawi, C., Sakka Hlaili, A., Tesán Onrubia, J.A., Thomas, B., Thyssen, M., Zaaboub, N.,

23 Zouari, A., Garnier, C., 2023. Contamination of planktonic food webs in the

1 Mediterranean Sea: Setting the frame for the MERITE-HIPPOCAMPE oceanographic cruise
2 (spring 2019). *Marine Pollution Bulletin*, 189 (2023) 114765

3
4
5 <https://doi.org/10.1016/j.marpolbul.2023.114765>
6

7
8 Uurasjärvi, E., Pääkkönen, M., Setälä, O., Koistinen, A., Lehtiniemi, M., 2021. Microplastics
9
10 accumulate to thin layers in the stratified Baltic Sea. *Environmental Pollution* 268,
11
12 115700. <https://doi.org/10.1016/j.envpol.2020.115700>
13
14

15
16 Whitmore, B. M., and M. D. Ohman. 2021. Zooglider-measured association of zooplankton
17
18 with the fine-scale vertical prey field. *Limnol. Oceanogr.* 66: 3811–3827.
19
20
21 doi:10.1002/lno. 11920
22
23

24
25 Zayen, A., Sayadi, S., Chevalier, C., Boukthir, M., Ben Ismail, S., Tedetti, M., 2020.
26

27 Microplastics in surface waters of the Gulf of Gabes, southern Mediterranean Sea:
28
29 Distribution, composition and influence of hydrodynamics. *Estuarine, Coastal and Shelf*
30
31 *Science*, 242, 106832. <https://doi.org/10.1016/j.ecss.2020.106832>
32
33
34

35
36 Zhao, S., Zettler, E. R., Bos, R. P., Lin, P., Amaral-Zettler, L. A., & Mincer, T. J., 2022. Large
37
38 quantities of small microplastics permeate the surface ocean to abyssal depths in the
39
40 South Atlantic Gyre. *Global Change Biology*, 28(9), 2991–3006.
41
42
43
44 <https://doi.org/10.1111/gcb.16089>
45
46
47
48
49
50
51
52
53
54
55
56
57
58
59
60
61
62
63
64
65

Figure captions:

1
2
3
4
5
6 **Figure 1:** Distribution of detritus (brown bar), mesozooplankton (blue bar), and
7
8 microplastics (MPs, orange bar) at the surface and at the chlorophyll maximum layer (CML)
9
10 at the 10 stations of the MERITE-HIPPOCAMPE cruise (see presentation in the text, and
11
12 detailed information in Tedetti et al., 2023 and Fierro et al., 2023). Values in Log10 for
13
14 detritus and zooplankton, Log10 (x 100) for MPs. Red, pink and green lines are respectively
15
16 the vertical profiles of temperature, salinity and fluorescence.
17
18
19
20
21
22
23
24
25

26 **Figure 2:** Distributions of the different types of microplastics (MPs) between fibers.
27
28 fragments, films, polystyrenes and pellets. Top: Distributions of the different types of MPs
29
30 between fibers, fragments, films, polystyrenes and pellets at the surface and the chlorophyll
31
32 maximum layer (CML). Sample of St.3 at the surface is missing. Bottom: Distributions of MPs
33
34 in size fractions at stations St.1, St.10 and St.19 at the surface and at the CML.
35
36
37
38
39
40
41
42

43 **Figure 3:** Non-Metric Multi-Dimensional scaling (NMDS) on abundances of MPs, % of fibers
44
45 in MPs, zooplankton and detritus, and on ratios zooplankton / MPs and detritus / MPs. NC:
46
47 northern coastal stations (St.3 is missing in surface waters); SC southern coastal stations; DS:
48
49 Deep-oceanic stations; Open symbols: Surface samples; Full symbols CML samples.
50
51
52
53
54
55
56
57
58
59
60
61
62
63
64
65

Table 1: Values of environmental variables (temperature, salinity, density, chlorophyll-*a*), concentration of detritus, zooplankton and microplastics (MPs), and ratios detritus/ MPs and zooplankton/MPs at the CML and at the surface. Zooplankton, detritus and MPs collected with Hydrobios 60 μm and then sieved > 200 μm at the CML, and collected with Manta net tow and sieved > 300 μm at the surface.

Zones	North Coast Stations				Deep Oceanic stations			South Coast Stations				
Stations	St1	St2	St3	St4	St9	St10	St11	St15	St17	St19	Mean	SD
Isobath (m)	91	1770	100	58	2575	2791	1378	100	50	50		
Surface												
Temperature ($^{\circ}\text{C}$)	14.9	14.0	14.2	13.9	14.3	15.5	15.3	17.3	17.2	17.8		
Salinity (‰)	38.1	37.9	37.8	38.1	38.4	37.5	37.4	37.3	37.5	37.6		
Density ($\times 1000 \text{ g l}^{-1}$)	28.4	28.4	28.3	28.6	28.7	27.8	27.7	27.2	27.4	27.3		
Chlorophyll- <i>a</i> (mg Chla m^{-3})	0.34	0.24	0.08	0.54	1.39	0.10	0.15	0.05	0.02	0.11		
Manta net Fraction > 300 μm												
Zooplankton (ind m^{-3})	6216	563	1573	3948	4224	1037	7069	4208	133	3307	3228	2366
Detritus ($\# \text{ m}^{-3}$)	8014	1893	4382	14742	2646	2543	378	2322	448	1725	3909	4393
Microplastics (MPs) ($\# \text{ m}^{-3}$)	2.3	0.7		0.2	0.1	0.1	3.0	3.4	0.2	0.3	1.1	1.4
Ratio Zoo/MPs	2652	759		20718	82368	13666	2395	1242	856	11467	15125	26193
Ratio Det /MPs	3418	2554		77365	51595	33522	128	685	2894	5983	19794	28080
CML depth	20-30m	25-35m	50-60m	30-40m	15-25m	45-55m	40-50m	65-75m	35-45m	35-45m		
Temperature ($^{\circ}\text{C}$)	14.3	13.8	13.7	13.7	14.2	14.6	15.2	15.1	16.7	17.0		
Salinity (‰)	38.1	38.2	38.2	38.2	38.4	37.8	37.4	37.4	37.5	37.8		
Density ($\times 1000 \text{ g l}^{-1}$)	28.5	28.7	28.8	28.7	28.8	28.2	27.8	27.8	27.5	27.6		
Chlorophyll- <i>a</i> (mg Chla m^{-3})	0.55	0.65	0.36	0.76	1.37	0.26	0.16	0.35	0.10	0.41		
Hydrobios – Fraction > 200 μm												
Zooplankton (ind m^{-3})	11312	567	2017	8643	2956	2106	727	346	12403	37474	7855	11363
Detritus ($\# \text{ m}^{-3}$)	40601	30532	68837	248097	41005	22355	16043	2508	342449	118535	93096	113514
Microplastics (MPs) ($\# \text{ m}^{-3}$)	68.6	117.9	31.9	43.4	12.1	16.8	10.1	11.7	50.7	34.5	39.8	33.5
Ratio Zoo/MPs	165	5	63	199	244	125	72	30	245	1086	223	315
Ratio Det /MPs	592	259	2158	5717	3389	1331	1588	214	6754	3436	2544	2268

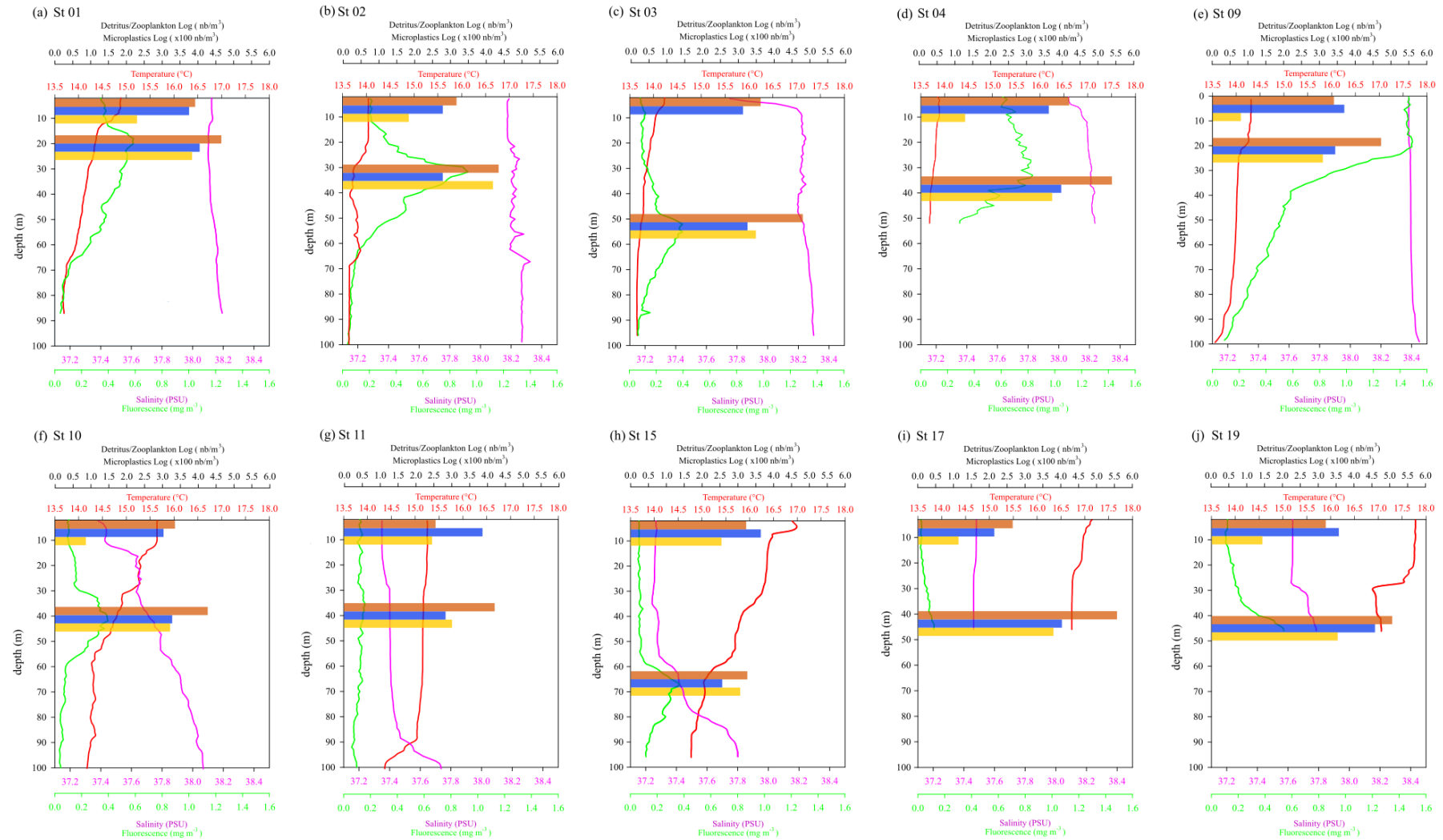


Figure 1: Distribution of detritus (brown bar), zooplankton (blue bar), and microplastics (MPs, orange bar) at the surface and at the chlorophyll maximum layer (CML) at the 10 stations of the MERITE-HIPPOCAMPE campaign (see presentation in the text, and detailed information in Tedetti et al., 2023 and Fierro et al., 2023). Values in Log10 for detritus and zooplankton, Log10 (x 100) for MPs. Red, pink and green lines are respectively the vertical profiles of temperature salinity and fluorescence.

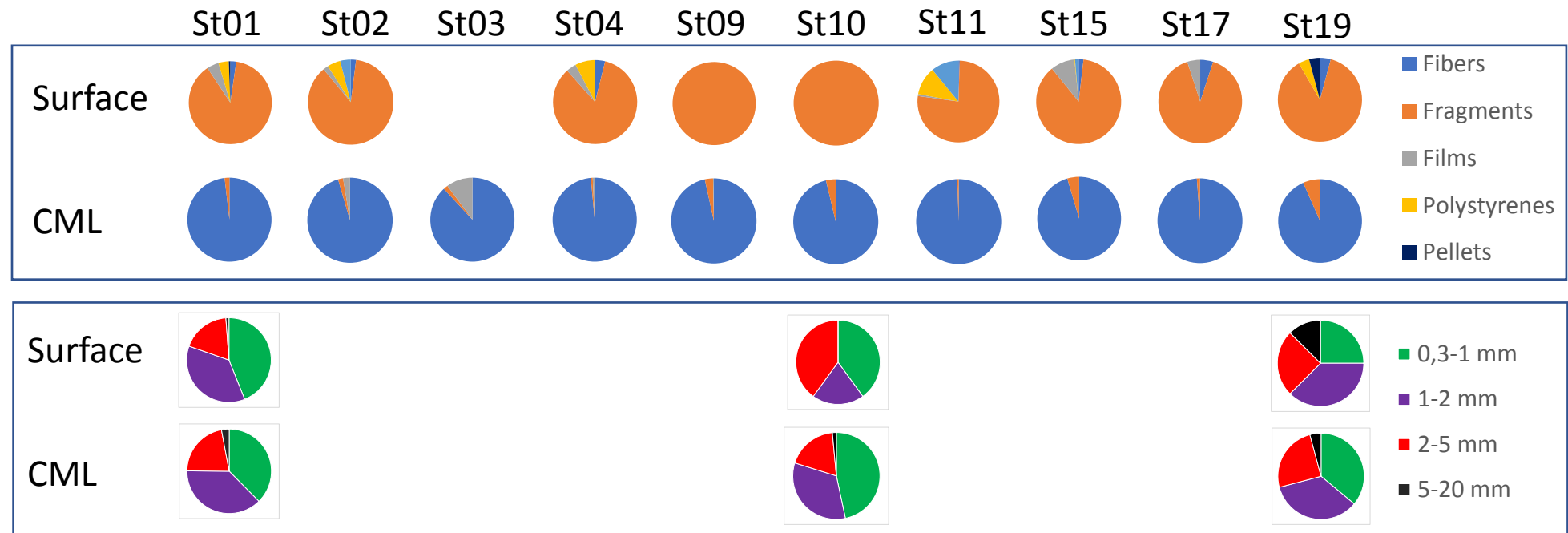


Figure 2: Distributions of the different types of microplastics (MPs) between fibers, fragments, films, polystyrenes and pellets. Top: Distributions of the different types of MPs between fibers, fragments, films, polystyrenes and pellets at the surface and the chlorophyll maximum layer (CML). Sample of St.3 at the surface is missing. Bottom: Distributions of MPs in size fractions at stations St.1, St.10 and St.19 at the surface and at the CML.

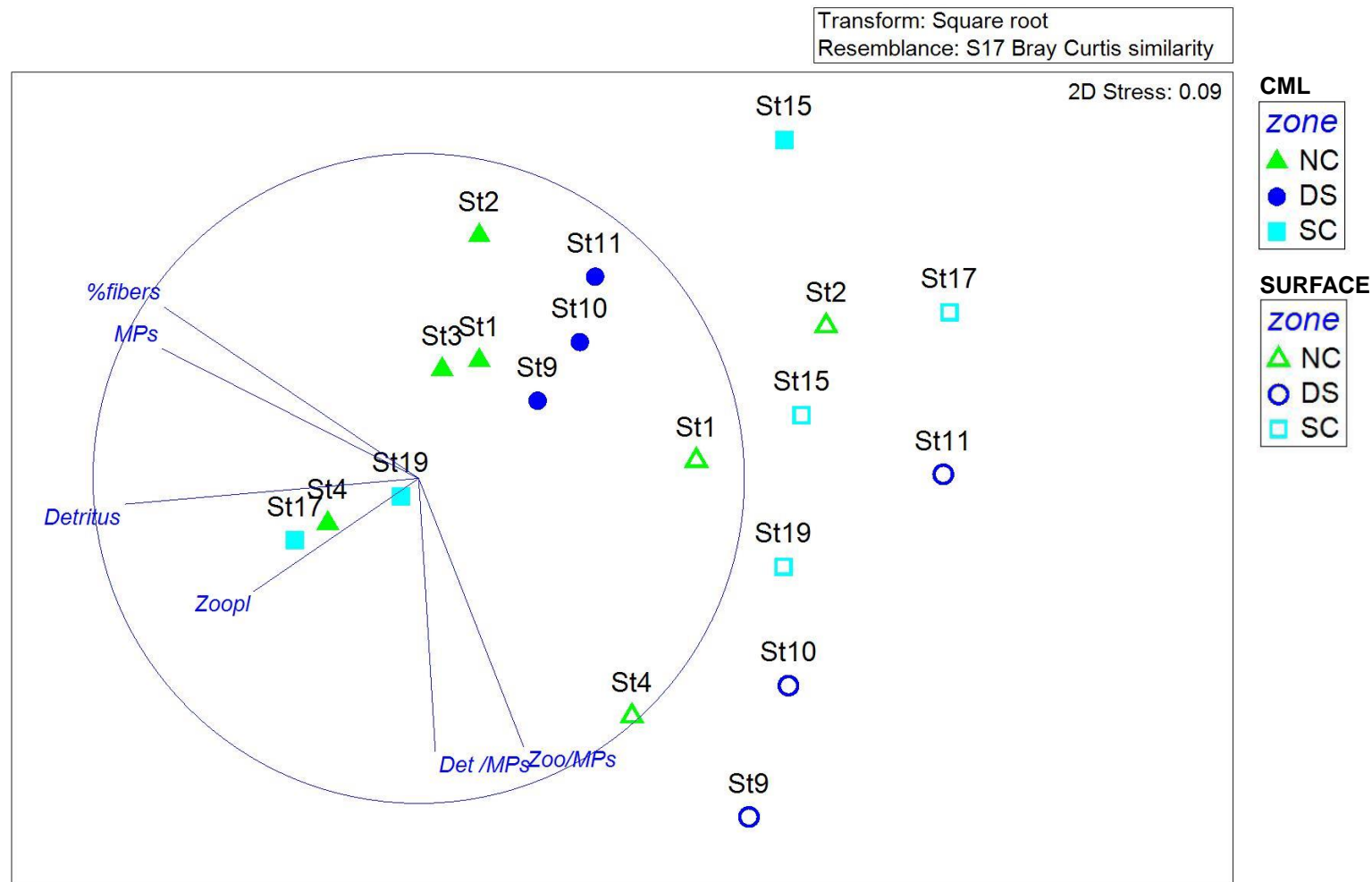


Figure 3: Non-Metric Multi-Dimensional scaling (NMDS) on abundances of MPs, % of fibers in MPs, zooplankton and detritus, and on ratios zooplankton / MPs and detritus / MPs. NC: northern coastal stations (St.3 is missing in surface waters); SC southern coastal stations; DS: Deep-oceanic stations; Open symbols: Surface samples; Full symbols CML samples.

Supplementary Material 1: Comparison of sampling efficiency of the two different sampling gears (Manta net with 300 µm mesh for surface layer sampling and 60µm mesh Multinet for horizontal CML sampling) for MP categories and size classes.

This additional material reproduces the detailed response to one of the reviewers on the comparability of the used two sampling gears and mesh sizes of the nets.

The Hippocampe cruise (and the scientific program of the same name) focused on organic and metallic contaminants in plankton collected at maximum chlorophyll.

In addition, Manta nets (300 µm mesh size) were programmed to quantify surface microplastics according to MSFD standards (Hanke et al., 2013). Initially, during our analysis of zooplankton communities from Hydrobios samples (60 µm) collected at maximum chlorophyll of the various stations (Fierro et al., 2023), a few microplastics items were observed in the aliquots studied for zooplankton treatment and identification with both Zooscan and binocular loupe. The idea then occurred to us to attempt to exhaustively quantify the microplastics after fractioning on 300 µm sieve of these samples obtained with the Hydrobios (60 µm mesh) at maximum Chlorophyll, in order to compare them with the microplastics data obtained using Manta net surface tows with a mesh size of 300 µm.

Obviously, the comparison is based on samples obtained using two different sampling protocols.

We will assess the impact of these differences below, but it is important to note the following similarities between the two approaches: 1) the volumes sampled by the two nets - Manta and Hydrobios - were fairly comparable (several tens of m³); 2) observations of microplastics in collected samples at the chlorophyll maximum layer (CML) with the Hydrobios (60 µm mesh size) was carried out on fractions sieved on 300 µm (to remain within the size range of the samples observed with the Manta), 3) the binocular loupe observation methods were similar.

The biggest problem in the comparison, raised by the reviewer, concerns the types of net and mesh used.

Hydrobios vs Manta net

The two nets have different characteristics, but can be used to sample very similar volumes of water. The Manta net (net opening 60 cm x 20 cm, mesh size 300 µm, IFREMER / MSFD protocol following Hanke et al. 2013) surfs over the water with its wings and the rectangular opening of the net mouth is designed to filter the first 10 cm of the surface layer of water. For each 10-minute stroke at 2 knots, the net filters approximately 100 m³. The Hydrobios type midi has an opening of 0.25 m² and can be towed to collect tens of m³, with real-time on-board control of the filtration level by the difference measured by 2 volumeters, one outside and one inside the net, which prevents clogging.

After the Hippocampe campaign (13 April - 14 May 2019), we organized a study in Marseille Bay to investigate the distribution of microplastics in the water column, using the same Multinet Hydrobios net and Manta net. This study, which was planned to take place over the different seasons of the same year (2020), was unfortunately halted by sudden restrictions on activities linked to the COVID pandemic. However, for two dates, we were able to obtain vertical distributions of microplastics under different wind conditions. These data supported simulations to investigate dynamic changes in the vertical distributions of microplastics and have been published (Chevalier et al., 2023 ; ; Chevalier, C., Vandenberghe, M., Pagano, M., Pellet, I., Pinazo, C., Tesán Onrubia, J.A., Guilloux, L., Carlotti, F., 2023. Investigation of dynamic change in microplastics vertical distribution patterns: The seasonal effect on

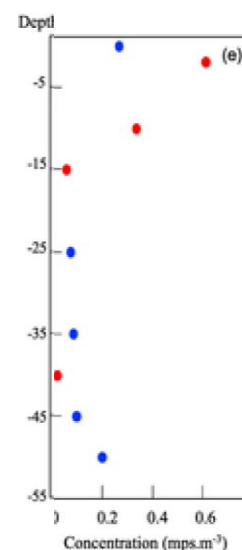
vertical distribution. *Marine Pollution Bulletin*, 189, 114674.
<https://doi.org/10.1016/j.marpolbul.2023.114674>).

The sampling conditions, the microplastics concentrations observed and the physical and chemical variables in the water column are presented in Table 1, Figure 3 and Table 2 respectively of the cited article (Chevalier et al., 2023).

In the table below, we have reproduced the microplastics concentration values by adding the % of fibers to the total PMs.

Date (dd.mm.yyyy)	Depth (m)	MPs concentration (mps/m ³)	% Fibers
03.02.2020 (blue dots on fig.)	0 (surface)	0.27	84,6 %
	25	0.08	33,3 %
	35	0.09	85,7 %
	45	0.1	37,5 %
	50	0.2	37,5 %
Water column MPs abundance (mps/m ²): 7.24			
10.02.2020 (red dots on fig.)	1	0.62	12,9 %
	10	0.34	52,9 %
	15	0.06	100 %
	40	0.02	100 %

Water column MPs abundance (mps/m²): 7,90



On 03.02.2020, with strong wind conditions (10 m/s) inducing mixing, due to turbulent vertical diffusivity (see Chevalier et al., 2023), the highest microplastics concentration was at the surface sampled with the 300 μ m mesh Manta net, and 84.6% of the MPs collected were fibers. Thus, the Manta net can collect fibers quite effectively (it sampled the highest percentage of fibers observed among the 9 analyzed samples). In the water column, the highest percentage of fibers was obtained at 35 m in an area where turbulent vertical diffusivity was low. On 10.02.2020, wind conditions were calm, and turbulent vertical diffusivity was low and homogeneous vertically. The MPs profile decreased drastically with depth, but the fiber contribution increased to reach 100% at 15m and 40m.

These data were used to calibrate and validate the model of the vertical distribution of microplastics as a function of wind conditions and made it possible to deliver consistent simulations that explain the observed distributions (see Chevalier et al., 2023).

Conclusion on the comparison of the two gears: On this basis, we do not consider that the use of the Hydrobios midi net versus Manta net induced major differences in the sampling process. In any case, at present, no other better combination of nets allows the surface and deep layers to be sampled horizontally with such precision, and with comparable collected samples in terms of filtered volumes. (Note that on 10.02.2020, the Hydrobios net was tested close to the surface (1m), but could not sample just the water surface interface.)

300 μ m mesh nets vs. 60 μ m mesh nets.

We used 300 μ m mesh for the Manta net and 60 μ m mesh for the Hydrobios during the Hippocampe cruise. However, our observation of the microplastics in the Hydrobios samples only concerned the fractions sieved above 300 μ m, in order to be able to compare them with the surface microplastics content in the Manta.

The effect of the mesh may have a different impact on the types of MPs depending on their shape, from round (such as pellets) to tapered (such as fiber-type).

Non-tapered microplastics (pellets, fragments, films, etc.) were retained either by the 300 μm mesh of the Manta, or by the 300 μm sieve of the samples collected from the 60 μm Hydrobios. It may be considered that that the collection efficiency in the two cases is very similar. Questions may arise for fibre-type microplastics: 1) Can fibers be correctly collected using a Manta net with a mesh size of 300 μm mesh? 2) Does collection by the Hydrobios with a net of 60 μm mesh allow more microplastics fibers to be collected, even those obtained after sieving with a 300 μm mesh?

The size of microplastic fibres (MFs) is highly variable due to their myriad sources, material types and degradation history. However, their diameter ranges from 10 to several tens of μm (average around 25-30 μm), and their length is usually 1 to 2 orders of magnitude greater than the diameter (Cole, 2016) (although the theoretical minimum length should be at least 3 times the value of the diameter). It is therefore conceivable that isolated fibers could almost all pass through a 300 μm mesh and most through a 60 μm mesh. In reality, because of the aggregation of microfibers with particles (phytoplankton aggregates, TEP, others) (Galgani et al. 2022), the retention of microfibers by a mesh depends more on the size of the particle in which the microplastics fiber is embedded.

In the observations made in the bay of Marseille in February 2020 and described above, fibers represented 84.6% of the microplastics collected at the surface with the Manta net on 3 February, and the surface had the highest concentration of microplastics among the layers sampled.

Conclusion on the effectiveness of the net meshes used: The 300 μm mesh Manta net is able to collect microplastics fibers with diameters much smaller than 300 μm , because they are most often found with marine snow, or aggregated with the plankton collected by the net. The 300 μm sieve used to fractionate the samples obtained with the Hydrobios 60 μm mesh net retains microplastics fibers in the same way.

Conclusion on this question: We believe that the methodology used enables us to propose a valid comparison of surface data and the CML microplastics content collected above a 300 μm mesh. However, a new dedicated experiment should focus on the use of nets with identical mesh sizes. It may be added that a true comparison would probably require more than just a comparison between nets and meshes, but also for different wind and vertical hydrodynamic conditions, and for different particle and microplastics distributions, and for different particle sizes.

References :

Cole M., 2016, A novel method for preparing microplastic fibers, *Scientific Reports*, 6 : 34519.

Galgani L., Goßmann I., Scholz-Böttcher B., Jiang X., Liu Z., Scheidemann L., Schlundt K., Engel A., 2022. Hitchhiking into the Deep: How Microplastic Particles are Exported through the Biological Carbon Pump in the North Atlantic Ocean. *Environmental Science & Technology* **2022** 56 (22), 15638-15649. DOI: 10.1021/acs.est.2c04712

Supplementary Material 2: **Examples of photographs of fibers, fragments and films found in our samples at the CML during the Hippocampe cruise**

Plate with examples of photos taken with a binocular magnifying glass to identify and measure microplastics in plankton samples collected at the CML.

